Extended Abstracts of the 2012 International Conference on Solid State Devices and Materials, Kyoto, 2012, pp470-471

PS-14-11

Carrier Transport Property of Heavily-Boron-Doped Degenerate Diamond Single-crystalline Thin Layers Etched with Hydrogen Plasma

Tomohiro Kuki, Osamu Maida and Toshimichi Ito

Graduate School of Engineering, Osaka University,
E-mail: kuki@daiyan.eei.eng.osaka-u.ac.jp

1. Introduction

Diamond is an attractive semiconductor because of its excellent properties such as very high breakdown electric fields, very high thermal conductivities, high electron and hole mobilities, and so on [1]. However, high-quality boron-doped CVD diamond films are indispensable for possible device applications. Unfortunately, the accepter level of B atoms substitutionaly located in diamond, the only one kind of dopants that can be rather well-controlled in diamond, is very deep (0.37 eV). Therefore, the available carrier density at room temperature is extremely low, compared to the other conventional *p*-type semiconductors having the same dopant density. When heavily B-doped (HBD) samples are grown, the carrier mobility seriously decreases much more strongly than in other semiconductors. Therefore, the heavily doping process of B atoms which can suppress the reported decreases in the hole mobility is one of the key issues.

HBD diamond films provide a metallic behavior while the carrier mobility observed is rather low, which is considered to originate from an impurity band conduction. Since the formation of such an impurity band in a semiconductor strongly depend on the density and thickness, the transport properties should depend on the thickness of HBD layers and their B densities. In the present study, thus, we have investigated dependences of the electronic transport property on the film thickness and B atomic density of HBD layers.

2. Experiments

High-pressure/high-temperature-synthesized (HPHT) Ib vicinal (001) substrates were used. The misorientation angle was 5°. After a series of cleaning processes [2,3], an undoped diamond layer was homoepitaxially grown as a buffer layer on a cleaned substrate using a high-power-density MWPCVD method with a source gas of H_2-diluted CH_4 (C/H ratio = 4.0 %). Then, thin B-doped layers were homoepitaxially deposited using H_2-diluted $B(CH_3)_3$ with B/C ratio of 8000 ppm or 12000 ppm. In order to vary the film thickness of the HBD layer, they were etched with hydrogen plasma, which was commonly employed for the epitaxial growth of high-quality diamond. After some measurements, an undoped diamond layer was homoepitaxially grown as a carrier transfer layer on a B-doped layer.

The surface morphology of these specimens was characterized by using a Nomarski-type optical microscope (OM), an atomic force microscope (AFM) and a scanning electron microscope (SEM). Steady-state cathodoluminescence (CL) spectra were measured at room temperature (RT) to obtain electronic information on the crystalline quality of undoped and HBD layers. Galvanomagnetic data were obtained through AC Hall-effect measurements based on the van der Pauw method [4].

3. Results and Discussion

Thin HBD layers were grown for 2 minutes with a source gas containing B/C ratios of 8000 ppm (called as Sample #1) and 12000 ppm (Sample #2). Fig. 1 shows temperature dependences of (a) the sheet resistance, (b) sheet Hall coefficient and (c) Hall mobility taken from Samples #2. Both the sheet resistance and sheet Hall coefficient of these as-grown HBD layers had almost no temperature dependences in the low temperature regions below ≈300 K and ≈180 K, respectively, demonstrating the presence of a metallic conduction in these HBD layers, as expected. Then, Samples #1 and #2 were exposed to hydrogen plasma to slightly etch the samples. With the increase of the etching time, the carrier density decreased while the carrier mobility increased. When the peaks disappeared in both temperature dependences of sheet Hall coefficients, the sheet resistance obtained for both samples increased with decreasing temperature, demonstrating a typical semiconducting behavior. This means that the electronic state in both HBD layers giving an impurity band conduction before the H-plasma etching was sufficiently localized after the etching so that the so-called impurity band conduction almost disappeared. These Hall data can be analyzed in detail, based on a two-type-carrier transportation model which considers both an impurity band and the valence bands composed of a light-hole band and two heavy-hole bands in diamond [5]. The effective activation energy deduced for Sample #1 was 0.27 eV, reducing from 0.37 eV, the typical activation energy of the accepter level of B atoms lightly doped in

diamond.

Fig. 2 shows the effect of the undoped overlayer grown on the localized HBD layers formed after the etching. As shown in Fig. 2 (c), the Hall mobility of Sample #1 increased by about 10 % after the growth of an undoped diamond overlayer. This indicates the carrier was likely to diffuse from the B-doped layer to the undoped layer. On the other hand, the Hall mobility of Sample #2 did not clearly increase after the growth of an undoped diamond overlayer. The possible origin may be attributed to the absence of substantially metallic region. In such a situation, the carriers hardly diffused to the undoped overlayer. This well correlates to the fact that the activation energy of Sample #2 was 0.35 eV close to the accepter level (0.37 eV) obtained for lightly B-doped samples.

Acknowledgement

This work was partly supported by the JSPS, Grant-in-Aid for Scientific Research (A) (21246011) and Grant-in-Aid for Young Scientists (B) (22760300).

References

[1] M.A. Prelas, G. Popovici, L.K. Bigelow (Eds.), "Handbook of Industrial Diamonds and Diamond Films", (Marcel Dekker, New York, 1998).

[2] O. Maida, H. Miyatake, T. Teraji and T.Ito, Diamond Relat. Mater. **17** (2008) 435.

[3] T. Nakai, K. Arima, O. Maida and T. Ito, J. Cryst. Growth **309** (2007) 134.

[4] L. J. van der Pauw, Philips Tech. Rev. **20** (1958) 220.

[5] M.Aono, O. Maida and T. Ito: Diamond Relat. Mater. **20** (2011) 1357.

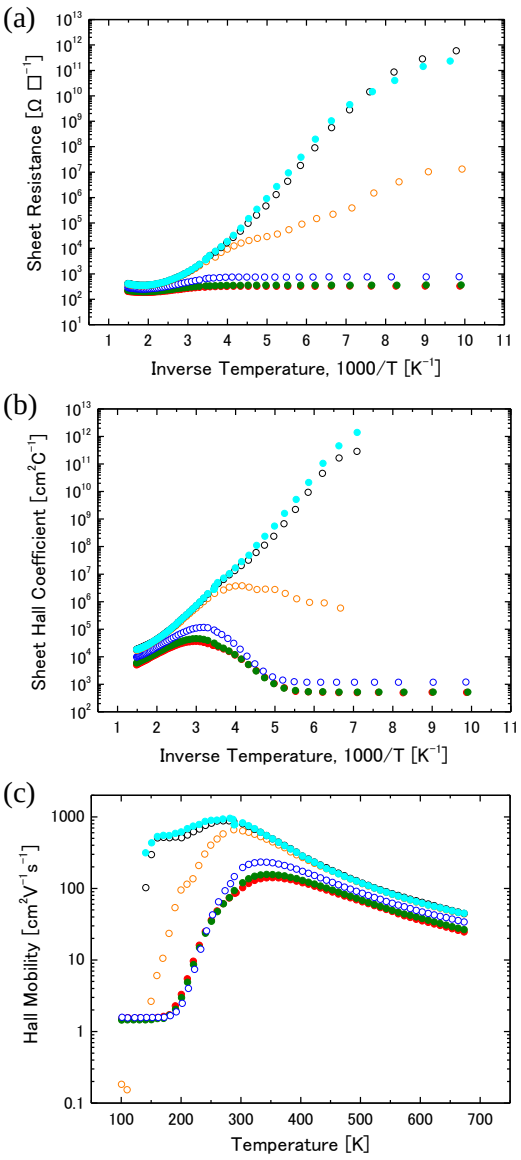

Fig. 1. Temperature dependences of (a) the sheet resistance, (b) sheet Hall coefficient and (c) Hall mobility taken from Sample #2 (etching time : ● 0- min, ● 5- min, ○ 10- min, ○ 20- min, ○ 30- min, ● 40- min).

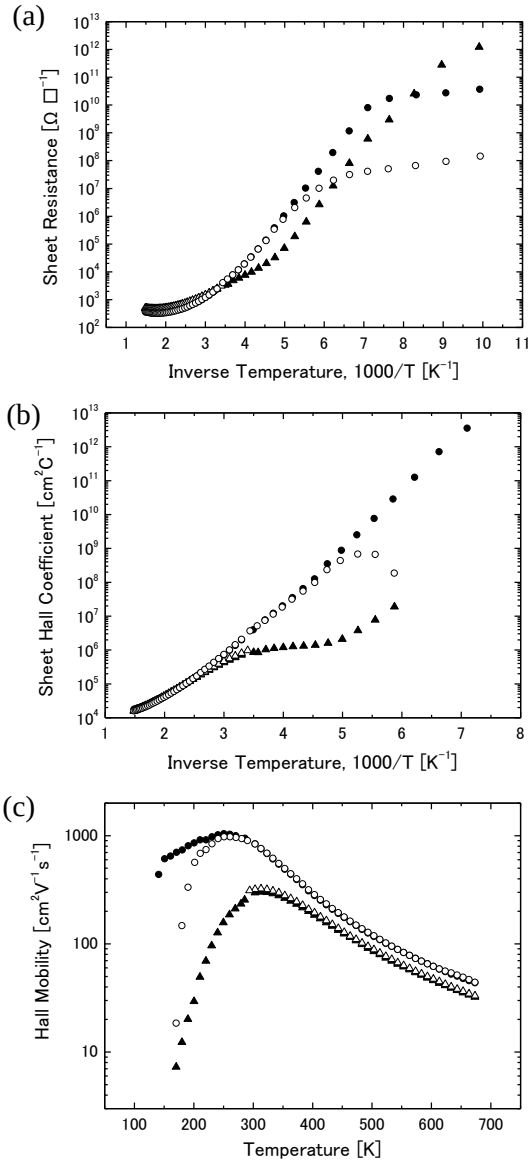

Fig. 2. Temperature dependences of (a) the sheet resistance, (b) sheet Hall coefficient and (c) Hall mobility taken from Sample #1 (▲90-min etching, △ undoped overlayer) and Sample #2 (●50-min etching, ○ undoped overlayer).